

热镀锌双相钢点焊结构的临界试样厚度

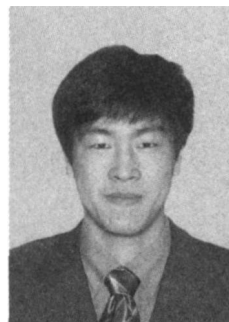
杨洪刚, 张延松, 来新民, 陈关龙

(上海交通大学 机械与动力工程学院, 上海 200240)

摘 要: 针对热镀锌双相钢 DP600 电阻点焊结构的分界面断裂失效, 利用统计分析方法, 研究了不同熔核长度(5~8 mm)下, 板厚分别为 0.8 mm 和 1.5 mm 的 DP600 点焊结构拉剪测试失效模式, 建立 DP600 点焊结构发生分界面断裂失效的概率与熔核长度和板厚的关系模型, 从而确定其临界试样厚度, 以及熔核长度对临界试样厚度的影响。结果表明, 熔核长度和板厚对 DP600 点焊结构分界面断裂失效的影响较大, 随着熔核长度的递增, 临界试样厚度呈线性增加。研究结果可为车身用高强钢电阻点焊结构的优化提供指导。

关键词: 电阻点焊; 双相钢; 分界面断裂; 临界试样厚度

中图分类号: TG407 文献标识码: A 文章编号: 0253-360X(2008)01-0093-04



杨洪刚

0 序 言

近年来, 随着人们对环境问题的认识和对安全性能要求的不断提高, 汽车车身构造和所用材料正在发生巨大变化。为了提高汽车行驶的经济性, 减轻汽车重量、降低燃油消耗和减少排放污染已成为世界汽车工业发展的核心问题。以高强钢为代表的材料, 由于其材料特性的提高以及经济性上的优势, 较好地适应汽车工业发展的新要求, 目前已在汽车车身、底盘、悬架、转向等零部件上广泛应用, 将成为未来汽车材料的中坚力量^[1-4]。

由于具有高抗拉强度、低屈服强度、且容易成形和耐蚀性好等优点, 高强钢中的热镀锌双相钢已成为目前各生产厂商研发的重点之一。然而, 由于双相钢自身材料性能的特点, 其电阻点焊结构往往发生分界面断裂失效, 尤其是较厚的板材。发生分界面断裂失效时, 点焊结构所能承受的载荷和碰撞时所消耗的能量均相对较小。研究表明, 与材料成分和锌层厚度的影响相比, 焊接工艺参数和板厚是影响熔核尺寸和分界面断裂失效的主要因素^[4]。为此, 文中利用统计分析方法, 通过对双相钢点焊结构拉剪测试失效模式的分析, 建立了双相钢点焊结构分界面断裂失效概率与板厚和熔核长度的关系模型, 并确定其临界试样厚度, 以及熔核长度对临界试样厚度的影响, 为高强钢点焊结构的优化及其在车身结构应用中的进一步推广提供指导。

1 试验系统与分析方法

1.1 试验系统

试验材料为美国通用公司提供的热镀锌双相钢 DP600, 其力学性能如图 1 所示。通常, 影响焊点拉剪强度测试的因素主要有焊点的质量、尺寸、位置以及试样的厚度、长度、宽度和搭接尺寸。其中, 试样的长度影响较小, 而且搭接尺寸与试样宽度相等即可满足要求^[5]。因此, 试验中试样长度固定为 100 mm, 试样厚度分别为 0.8、1.5 mm, 且点焊时搭接尺寸与试样宽度相等。点焊试样均由 AC 型伺服焊枪制备完成。

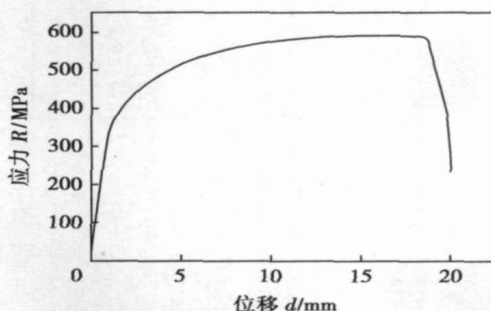


图 1 DP600 力学性能

Fig. 1 Mechanical property of DP600 steel

为了实现不同熔核长度的焊点, 试验中将端面直径分别为 5~8 mm 的球面平头电极两端进行铣削

加工, 并保证电极端面的宽度保持一致, 均为 4 mm, 如图 2 所示。通过调整焊接参数, 获得相应长轴长度的熔核, 对于不同的板厚, 每一个熔核长度分别完成八个点焊试样。试样的拉剪强度测试在 KDW-20 型微机控制电子万能试验机上进行, 试验中分别记录了相应的断裂失效模式。双相钢焊点的拉剪失效模式主要有分界面断裂和焊点拔出两种(图 3)。与分界面断裂相比, 焊点拔出时焊点周围发生塑性变形, 熔核能够吸收较多能量, 从而是一种较为理想的失效模式^[2, 9]。

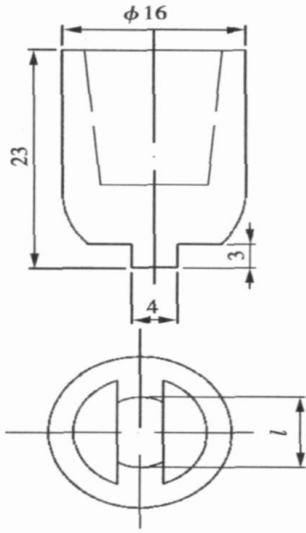


图 2 加工后的电极几何尺寸

Fig. 2 Geometry dimension of modified electrode tip

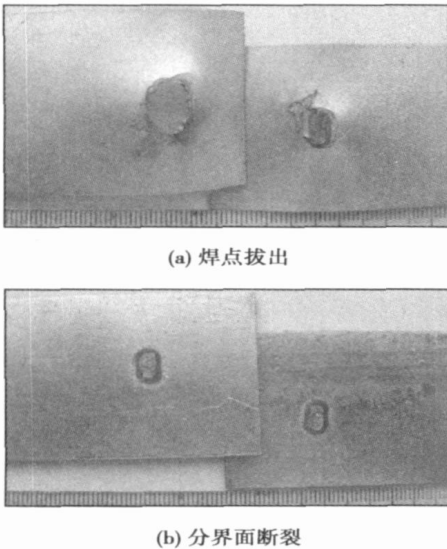


图 3 双相钢焊点主要的拉剪失效模式

Fig. 3 Primary failure modes of DP600 steel welding spots

1.2 统计分析方法

统计分析方法能够有效鉴别重要因素及其相互之间的影响, 并且能够建立用于预测结果和进一步分析的统计模型^[6, 7]。点焊试样的失效模式可分为分界面断裂模式和焊点拔出等非分界面断裂模式, 具有二分属性, 因而选用分析二分类变量时最常用的统计分析模型之一——logistic 回归模型。

在 logistic 模型中, 描述事件概率 P 和变量 x 之间的关系通常可表示为

$$\ln \frac{P}{1-P} = f(x) \tag{1}$$

式中: $f(x)$ 是 x 的实函数, 并且通常是 x 的多项式形式。文中主要目的是建立发生分界面断裂失效模式的概率 P 与熔核长度 l 和板厚 t 的函数关系, 即有两个输入变量, 熔核长度 l 和板厚 t 。因此 $f(x)$ 可表示为 $f(x) = a_0 + a_1l + a_2t + a_3lt + a_4t^2 + a_5l^2 + a_6lt^2 + a_7tl^2$ (2)

其中的系数可由试验数据进行评估。但是各多项式之间的相关性降低了系数评估的准确性, 因此需要通过 Gram-Schmidt 变换将多项式矢量 x 转换成正交矢量。

分别令 x_t, x_l 代表板厚和熔核长度的数据矢量, x_t^2, x_l^2 代表 x_t, x_l 的平方矢量, 且

$$u_l = x_l - (Ix_l^T)I, z_l = u_l / \|u_l\|$$

$$u_l^2 = x_l^2 - (z_l x_l^2)^T z_l - (Ix_l^2)^T I, z_l^2 = u_l^2 / \|u_l^2\| \tag{3}$$

其中 I 是单位矢量, $I = (1, 1, \dots, 1)$, T 表示矢量的转置。 z_l 表示熔核长度的线性影响, z_l^2 表示熔核长度的平方影响。图 4 显示了变换后熔核长度的线性影响和平方影响与原始矢量之间的关系。由图 4 可见,

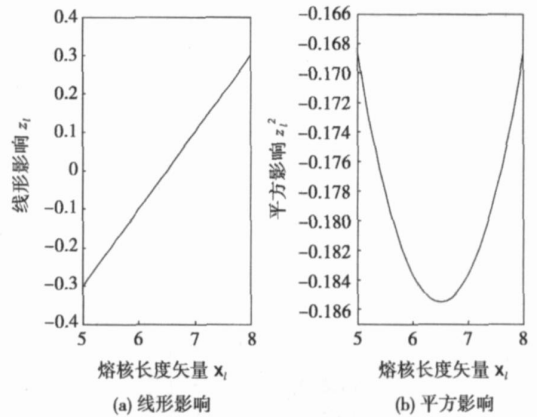


图 4 熔核长度正交变换前后的关系

Fig. 4 Relationship between original netget length and transformed netget length

$\{z_l, z_l^2\}$ 是正交的, 而且存在以下对应关系, 即

$$l_s = a_{10} + a_{11}l$$

$$l_s^2 = a_{20} + a_{21}l + a_{22}l^2 \quad (4)$$

其中 l_s 和 l_s^2 是 l 和 l^2 的多项式变换。对板厚 t 作类似的正交变换, 从而式(1)可转换为

$$\ln \frac{P}{1-P} = \theta_0 + \theta_1 l_s + \theta_2 t_s + \theta_3 l_s t_s + \theta_4 t_s^2 + \theta_5 l_s^2 + \theta_6 l_s t_s^2 + \theta_7 t_s l_s^2 \quad (5)$$

式中各多项式间具有较好的正交性, 因而系数的评定变得更加有效和相对独立, 使得回归模型也更加精确。将熔核长度和板厚变换前后的对应关系代入, 即可得到分界面断裂概率与原始矢量之间的函数关系。

2 试验结果与分析

2.1 分界面断裂失效概率函数

不同熔核长度和板厚下, 双相钢 DP600 点焊结构产生分界面断裂失效模式的概率如表 1 所示。板材较厚时发生分界面断裂失效的倾向较大, 而且随着熔核长度的增加, DP600 点焊结构发生分界面断裂失效的概率逐渐降低。经过上述正交变换和 logistic 回归分析, 可得 DP600 点焊结构发生分界面断裂失效的概率与熔核长度和板厚的函数关系模型为

$$\ln \frac{P}{1-P} = -82.2991504 + 13.1434022l + 88.170202t - 17.263910tl - 0.834775l^2 + 1.0842884t^2 = f(t, l) \quad (6)$$

对数变换后可得

$$P = e^{f(t, l)} / (1 + e^{f(t, l)}) \quad (7)$$

表 1 DP600 点焊结构分界面断裂失效概率

Table 1 Probability of interfacial fracture mode for DP600 steel welding spots

熔核长度 l / mm	板厚 t / mm	分界面断裂 概率 P (%)
5	0.8	0.0
5	1.5	100.0
6	0.8	0.0
6	1.5	87.5
7	0.8	0.0
7	1.5	37.5
8	0.8	0.0
8	1.5	25.0

2.2 熔核长度与临界试样厚度的关系

将熔核长度和板厚分别带入式(7), 可得到不同

熔核长度下 DP600 点焊结构发生分界面断裂失效的概率随板厚的变化规律(图 5)。针对双相钢 DP600 点焊结构, 定义发生分界面断裂失效概率为 100% 的转折点为分界面断裂失效的临界试样厚度, 如图中箭头所指。图 6 反映了熔核长度与临界试样厚度的关系, 可见, 随着熔核长度的递增, 临界试样厚度基本呈线性增加。通过增加熔核长度的方法, 可降低 DP600 点焊结构的分界面断裂失效, 保证焊接质量。

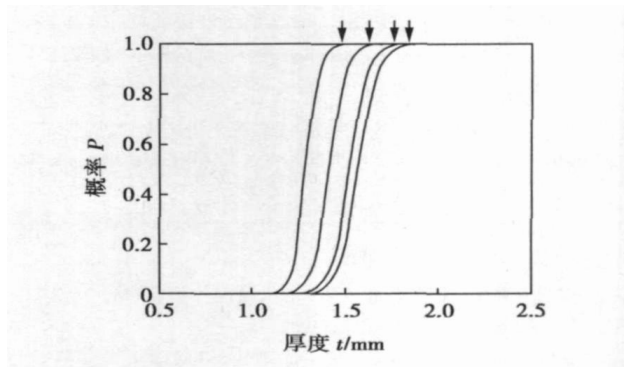


图 5 DP600 焊点分界面断裂失效概率

Fig. 5 Probability of interfacial fracture for DP600 steel welding spots

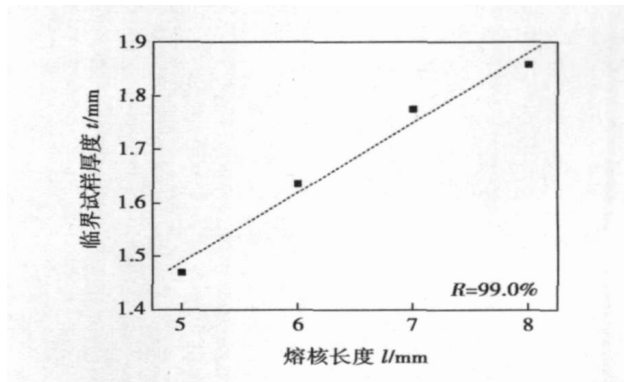


图 6 熔核长度与临界试样厚度的关系

Fig. 6 Relationship between length of nugget and critical specimen thickness

3 结 论

(1) 分析了不同熔核长度和板厚下, 热镀锌双相钢 DP600 点焊结构的拉剪测试失效模式, 结果显示熔核长度和板厚对 DP600 点焊结构分界面断裂失效具有较大影响。

(2) 通过 logistic 统计回归分析, 建立了 DP600 点焊结构发生分界面断裂失效的概率与熔核长度和板厚的函数关系模型。

(3) 针对 DP600 点焊结构分界面断裂失效, 提出了临界试样厚度的概念, 确定了熔核长度与临界试样厚度的关系。随着熔核长度的递增, 临界试样厚度呈线性增加。通过增加熔核长度, 可降低 DP600 点焊结构的分界面断裂失效。

参考文献:

- [1] Merklein M, Geiger M. New materials and production technologies for innovative lightweight constructions [J]. Journal of Materials Processing Technology, 2002, 125-126: 532-536.
- [2] Marya M, Gayden X Q. Development of requirements for resistance spot welding dual-phase DP600 steels [J]. Welding Journal, 2005, 85 (12): 197s-204s.
- [3] Zadeh L A. 模糊集合、语言变量及模糊逻辑 [M]. 陈国权, 译. 北京: 科学技术出版社, 1982.
- [4] 楼世博, 孙章, 陈化成. 模糊数学 [M]. 北京: 科学技术出版社, 1983.
- [5] 扈庐. 实用模糊数学 [M]. 北京: 科学技术出版社, 1989.
- [6] 中国现场统计研究会三次设计组编著. 正交法和三次设计 [M]. 北京: 科学技术出版社, 1985.
- [7] 葛苏林. 模糊子集模糊关系模糊映射 [M]. 北京: 北京师范大学出版社, 1985.
- [8] 汪培庄. 模糊集合论及其应用 [M]. 上海: 上海科学技术出版

- [3] 叶平, 沈剑平, 王光耀, 等. 汽车轻量化用高强度钢现状及其发展趋势 [J]. 机械工程材料, 2006, 30(3): 4-7.
- [4] 中国机械工程学会焊接学会. 焊接方法与设备焊接手册 (第 1 卷) [M]. 2 版. 北京: 机械工业出版社, 2002.
- [5] Sparagen W, Corbovi M A. Mechanical characteristics of resistance welds in plain carbon steels [J]. Welding Journal, 1944, 23(7): 305s-343s.
- [6] Zhou M, Zhang H, Hu S J. Critical specimen sizes for tensile shear test [J]. Welding Journal, 1999, 78(9): 305s-313s.
- [7] Zhang H, Hu S J, Senkara J, et al. A statistical analysis of expulsion in resistance spot welding [J]. ASME Journal of Manufacturing Science and Engineering, 2000, 122(3): 501-510.

作者简介: 杨洪刚, 男, 1979 年出生, 博士研究生。研究方向为高强度电阻点焊焊接质量在线监测与控制方法研究。发表论文 4 篇。

Email: hgyang@sjtu.edu.cn

[上接第 92 页]

- [9] Harrison J D. Basis for a proposed acceptance standard for weld defects 2: slag inclusions [J]. Metal Construction, 1972, 4(7): 262-268.
- [10] 荆树峰. 国外压力容器缺陷评定标准 [M]. 北京: 劳动出版社, 1982.

社, 1983.

- [9] Harrison J D. Basis for a proposed acceptance standard for weld defects 2: slag inclusions [J]. Metal Construction, 1972, 4(7): 262-268.
- [10] 荆树峰. 国外压力容器缺陷评定标准 [M]. 北京: 劳动出版社, 1982.

作者简介: 刘曦, 男, 1964 年出生, 博士, 高级工程师。主要从事机械方面的科研和教学工作。发表论文 20 余篇。

Email: liuxi1278069826@126.com

method was proposed, which adding median current between the two peaks of pulse current. And the welding process was tested and analyzed with independently self developed welding arc dynamic wavelet analyzer. The result showed that instantaneous short circuit occurs if the forward median current was too small. Contrarily, if it is too large, forward median waveforms will be hardly observed. The result also indicated that the median phase effect will not be obvious if the forward median time is too short, but the welding process will not be stable if it is too long. Controllability of droplet transfer can be realized by proper median current and median time. And the optimal matching parameters for pulse current and pulse time were given under this experiment conditions.

Key words: pulsed metal inert-gas welding; forward median waveform control; droplet transfer; wavelet analysis

Analysis of stability in droplet transfer process of GMAW based on self correlation

BAO Ailian¹, GENG Zheng², LIU Wanhui¹
(1. School of Materials Science and Engineering, Heilongjiang Institute of Science and Technology, Harbin 150027, China; 2. National Key Laboratory of Advanced Welding Production & Technology, Harbin Institute of Technology, Harbin 150001, China). p77—80

Abstract: Self-correlation analysis is an important analyzing method in signal analysis and processing. Some welding parameters attribute values, such as current, voltage etc, were acquired in GMAW (gas metal arc welding) process. The stability of droplet transfer process in GMAW and welding parameter were studied. Using time domain self-correlation character principle in digital signal analysis and processing, periodic property of welding current and voltage were identified. Through the acquired signal time domain periodic property, the stability of droplet transfer process in GMAW can be visually reflected.

Key words: gas metal arc welding; droplet transfer; self-correlation analysis; stability

Development of feature database of welded joint for the oil box based on Msc. Marc

GAO Jiashuang¹, YANG Jiang¹, LIU Xuesong¹, FANG Hongyuan¹, FU Wei²(1. State Key Laboratory of Advanced Welding Production Technology, Harbin Institute of Technology, Harbin 150001, China; 2. Shanghai Baosteel Group Corporation Baoshan Machineman Factory, Shanghai 201900, China). p81—84

Abstract: As the complexity and difficulty to create and mesh modeling of welded joint in Msc. Marc's preprocessing system, a feature database of welded joint for the kind of oil box was developed with Python language. Meanwhile a new menu system based on welded joint feature was also established with Marc's menu languages. These improvements of feature database and menu system make numerical simulation of welding process easier and design of welded joint faster. In addition, this method also provides good guidance of adding user special program into Marc and applying Chinese patch to Marc.

Key words: Marc; welded joint; menus; feature database

Welding residual stress of titanium vessel calculated by biaxial strength theory

CHEN Jiguang (Department of Civil Construction and Engineering, Hunan Institute of Science and Technology, Yueyang 414000, China). p85—88

Abstract: Titanium sheet has obvious orthogonal anisotropy and biaxial strengthening effect. Based on the biaxial strength theory, the formula for the welding residual stresses existed in the titanium pressure vessel were derived and the computation and analyses were carried out according to the experimental data. The result indicates that the longitudinal and surrounding residual stresses in longitudinal weld of the welding titanium vessel are greater 50% than the titanium sheet's yield strength. Moreover, the longitudinal and surrounding residual stresses in surrounding weld are extremely non-uniform. The numerical results show a wide difference, and the simulated values of some points are even minus values. Compared the titanium pressure vessel's experimental welding stresses with the calculated welding stresses, it is found that the most important surrounding stresses are basically consistent, and the greatest difference is less than 15%, which indicates that the computational method conforms with the real situation existed in titanium pressing pressure vessel.

Key words: biaxial strength theory; titanium pressure vessel; welding residual stress; formula

Fatigue reliability evaluation for welding construction containing welding defects

LIU Xi (Postdoctoral Research Department, Mechanical Engineering College, Nanjing University of Technology, Nanjing 210009, China). p89—92

Abstract: On the basis of the experiment, a synthesized evaluation of welding defects to fatigue strength of welding construction is made by fuzzy sets theory. The evaluation takes into account the interrelations among the category, dimension, location and the interaction of defects. Accordingly, a characteristic parameter $\mu(X)$ is proposed to evaluate the fatigue strength of welding construction containing defects. Combining this characteristic parameter $\mu(X)$ with the quality zone theory, a μ -S-N-P pattern is developed. The problems concerned by engineers such as how to calculate the reliability of welding construction containing defects can be solved when the status of defects is known. The characteristic parameter $\mu(X)$ coincides with the proposed primary fatigue source model.

Key words: welding defects; reliability evaluation; fuzzy sets theory; fatigue strength

Critical specimen thickness of hot galvanized dual-phase steel spot welding

YANG Honggang, ZHANG Yansong, LAI Xinmin, CHEN Guanlong (School of Mechanical Engineering, Shanghai Jiao Tong University, Shanghai 200240, China). p93—96

Abstract: Aiming at the interfacial fracture failure of resistance spot welding structure of hot galvanized steel DP600, the tensile failure modes of DP600 spot welding with different thickness (0.8 mm and 1.5 mm) and length of the nugget (5—8 mm) were studied through statistical analysis method. The relationship between the

probability of the interfacial fracture mode for DP600 welding spots and the thickness and the length of the nugget was also established. Then the critical specimen thickness was determined and the influence of the length of the nugget on the critical specimen thickness was investigated. The result shows that the thickness and the length of the nugget have great effect on the interfacial fracture mode of DP600 welding spots. And the critical specimen thickness linearly increased with the length of the nugget. The research result provides a theoretical guidance for the optimization of the structure of high strength steel resistance spot welding in automobile body.

Key words: resistance spot welding; dual-phase steel; interfacial fracture; critical specimen thickness

Automatic thickness measurement device for resistance welding machine HUANG Chao, SUN Dongming, HU Yongpeng (College of Mechanical and Electrical Engineering, Kunming University of Science and Technology, Kunming 650093, China). p97–100

Abstract: In order to adapt the development of the resistance welding technology and improve the automation of the resistance welding machine, an automatic thickness measurement device with the photoelectric coder and the PLC high-speed counter was studied based on the structure and application situation of the resistance welding machine. The type, construction, working principle of the photoelectric coder were especially introduced. And actual application in this thickness measuring device was expounded. This device can feed the measured data back to the controller of the welding machine automatically, then the best welding parameters correspond with the thickness of the weldment were chosen in advance in order that the welding machine can weld the work piece automatically in sequence. The experimental results indicate that this thickness measurement device can achieve the precision demand of choosing the welding parameters and can satisfy the actual production well.

Key words: resistance welding machine; thickness measurement; photoelectric coder; PLC high-speed counter

Effect of Fe particle parameter on coating build-up in low-temperature high velocity fuel spraying process YUAN Xiaojing¹, WANG Hangong¹, HOU Genliang¹, ZHA Bailin¹, YANG Junhua², WEI Zhitong³ (1. Xi'an Research Institute of Hi-Tech, Shanxi, Xi'an, 710025, China; 2. Staff of military deputy Xiaogan, Hubei, Xiaogan 432100, China; 3. 96272 Army, Luoyang 741023 Henan, China). p101–105

Abstract: Using LS-DYNA deformation dynamic response of finite element analysis coupling with structure and heat transfer, the impact behavior of Fe particle on the substrate (or previously deposited coating) was simulated in the low-temperature high-velocity air-fuel-spraying process. It shows that the temperature at the contact interface is increased with the increases of temperature and velocity of particle because the energy of particle increases. Synchronously, the plastic strain of particle changed so that the flatten particle can be obtained in this process. When the particles impact the substrate,

the substrate properties can determine the particle deposition and the adhesion of the coating to the substrate. During the coating building up, the deformation of deposited particle can result in the coarseness of the coatings surface so that the critical velocity of Fe particle can be decreased. The flying particle can impact on the deposited particle, which result in the second deformation and temperature variation of previously deposited coating. Because the temperature at the interface can't get to the Fe melting point, the coatings only present the mechanical adhesion. So, the brittle rupture is present at the tensile stress.

Key words: thermal spray; Fe coatings; particle parameter; numerical simulation

Artificial neural network to predict toughness parameter CVN of welded joint of high strength pipeline steel BAI Shiwu¹, TONG Lige², LIU Fangming³, WANG Li² (1. School of Materials Science and Engineering, Tianjin University, Tianjin 300072, China; 2. School of Mechanical Engineering, University of Science and Technology Beijing, Beijing 100083, China; 3. Pipeline Research Institute of China National Petroleum Corporation, Langfang 065000, China). p106–108

Abstract: The artificial neural network (ANN) model was developed with VC++ 6.0 based on multilayer back propagation (BP) to analyze and predict the Charpy-V notch (CVN) impact toughness parameter of the pipeline steel welded joint. Based on the practical welding parameters of X70 steel, the mean energy input, wall thickness, preheat temperature, welding position and sampling position were used as the input parameters of ANN, which includes one hidden layer with 14 nodes and Sigmoid activation function. The 194 sets of data, obtained from the practical welding, were divided randomly into two parts, in which 150 were used as training data and the other as testing data. The influence of structure of ANN on prediction results was analyzed. The number of the sample whose error is less than 20% is about 77% in the total testing data.

Key words: high strength pipeline steel; Charpy-V notch impact toughness parameters; artificial neural network

Effect of niobium on ductility drop cracking susceptibility of nickel-base alloys TANG Zhengzhu, CHEN Peiyin, WU Wei (Harbin Welding Institute, Harbin 150080, China). p109–112

Abstract: The strain-to-fracture was used to determine the strain threshold and temperature which cause cracking and quantify the DDC (ductility dip cracking) susceptibility of HS690 filler metals which have different content of Nb. The morphology and distribution of precipitation was analyzed by transmission electron microscope. The results show that adding Nb to HS690 filler metal will improve the quantity and morphology of the second phase (Nb, Ti)C in grain boundaries, the condition of grain boundaries and DDC susceptibility of HS690 filler metal.

Key words: nickel-base alloys; strain to fracture; ductility drop cracking; second phase